Chemical and Kinetic Reaction Mechanisms of Quinohemoprotein Amine Dehydrogenase from *Paracoccus denitrificans*†

Dapeng Sun,‡ Kazutoshi Ono,§ Toshihide Okajima,§ Katsuyuki Tanizawa,§ Mayumi Uchida,|| Yukio Yamamoto,|| F. Scott Mathews,⊥ and Victor L. Davidson*,‡

Department of Biochemistry, University of Mississippi Medical Center, Jackson, Mississippi 39216-4505, Institute of Scientific and Industrial Research, Osaka University, Ibaraki, Osaka 567-0047, Japan, Graduate School of Human and Environmental Studies, Kyoto University, Kyoto 606-8501, Japan, and Department of Biochemistry and Molecular Biophysics, Washington University School of Medicine, St. Louis, Missouri 63110

Received June 19, 2003; Revised Manuscript Received July 25, 2003

ABSTRACT: Quinohemoprotein amine dehydrogenase (QHNDH) possesses a cysteine tryptophylquinone (CTQ) prosthetic group that catalyzes the oxidative deamination of primary amines. In addition to CTQ, two heme *c* cofactors are present in QHNDH that mediate the transfer of the substrate-derived electrons from CTQ to an external electron acceptor. Steady-state kinetic assays yielded relatively small k_{cat} values ($<6\ s^{-1}$), and the rate-limiting step appears to be the interprotein electron transfer from heme in QHNDH to the external electron acceptor. Transient kinetic studies of the CTQ-dependent reduction of heme in QHNDH by amine substrates yielded different rate constants for different substrates (72, 190, and 162 s^{-1} for methylamine, butylamine, and benzylamine, respectively). Deuterium kinetic isotope effect (KIE) values of 5.3, 3.9, and 8.5 were observed, respectively, for the reactions of methylamine, butylamine, and benzylamine. These results suggest that the abstraction of a proton from the α-methylene group of the substrate, which occurs concomitant with CTQ reduction, is the rate-limiting step in the CTQ-dependent reduction of hemes in QHNDH by these amine substrates. In contrast, the reaction of 2-phenylethylamine with QHNDH does not exhibit a significant KIE ($^{H}k_3/^{D}k_3 = 1.05$) and exhibits a much smaller rate constant of 16 s^{-1}. This suggests that for 2-phenylethylamine, the rate-limiting step in the single-turnover reaction is either hydrolysis of the imine reaction intermediate from CTQ or product release prior to intraprotein electron transfer. Analysis of the products of the reactions of QHNDH with chiral deuterated 2-phenylethylamines demonstrated that the enzyme abstracts the pro-*S* proton of the substrate in a highly stereospecific manner. Inspection of the crystal structure of phenylhydrazine-inhibited QHNDH suggests that $Asp33_\gamma$ is the residue that performs the proton abstraction. On the basis of these results, kinetic and chemical reaction mechanisms for QHNDH are proposed and discussed in the context of the crystal structure of the enzyme.

Quinohemoprotein amine dehydrogenase (QHNDH)[1] is a periplasmic enzyme that has been isolated from *Pseudomonas putida* (*1*) and *Paracoccus denitrificans* (*2*). QHNDH expression is induced during growth with long carbon chain primary amines such as butylamine, as well as with benzylamine or 2-phenylethylamine as the sole source of carbon and energy (*1*−*3*). QHNDH catalyzes the oxidative deamination of a primary amine to generate the corresponding aldehyde plus ammonia. After substrate oxidation, QHNDH catalyzes a series of intraprotein electron transfer (ET) reactions between its three redox cofactors and then interprotein ET of the substrate-derived electrons to its physiological electron acceptor, cytochrome *c*-550 in *P. denitrificans* (*4*) or azurin in *Ps. putida* (*1*). In *P. denitrificans*, cytochrome *c*-550 mediates the electron transfer from QHNDH to the membrane-bound respiratory chain, most probably to cytochrome *c* oxidase (*4*).

QHNDH is an $\alpha\beta\gamma$ heterotrimeric protein. Crystal structures of QHNDH from *P. denitrificans* (*5*) (PDB entry 1JJU) and *Ps. putida* (*6*) (PDB entry 1JMX) are available. The smallest 82-residue γ subunit contains a novel redox cofactor, cysteine tryptophylquinone (CTQ) (Figure 1), which consists

† This work was supported by NIH Grant GM41574 (V.L.D.), NSF Grant MCB-00091084 (F.S.M.), Grants-in-Aid from the Ministry of Education, Culture, Sports, Science and Technology of Japan (Priority Areas, No. 13125204; the 21st Century COE Program), and a Research Grant from the Japan Society for the Promotion of Science (Category B, No. 12480180) (K.T.).

* To whom correspondence should be addressed. Phone: (601) 984-1516. Fax: (601) 984-1501. E-mail: vdavidson@biochem.umsmed.edu.

‡ University of Mississippi Medical Center.

§ Osaka University.

|| Kyoto University.

⊥ Washington University School of Medicine.

[1] Abbreviations: QHNDH, quinohemoprotein amine dehydrogenase; ET, electron transfer; CTQ, cysteine tryptophylquinone; TTQ, tryptophan tryptophylquinone; MADH, methylamine dehydrogenase; AADH, aromatic amine dehydrogenase; E_m, oxidation−reduction midpoint potential; PES, phenazine ethosulfate; PMS, phenazine methosulfate; DCIP, 2,6-dichlorophenolindophenol; KIE, kinetic isotope effect; Phz, phenylhydrazine; Trq, tryptophylquinone.

10.1021/bi035062r CCC: $25.00
Published on Web 08/26/2003

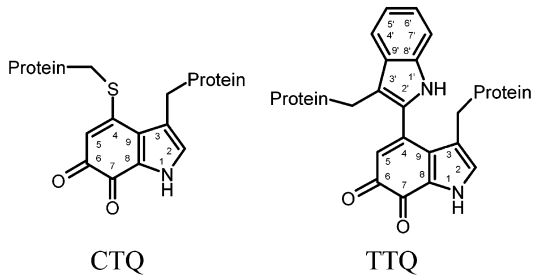

FIGURE 1: Oxidized forms of the cysteine tryptophylquinone (CTQ) and tryptophan tryptophylquinone (TTQ) cofactors.

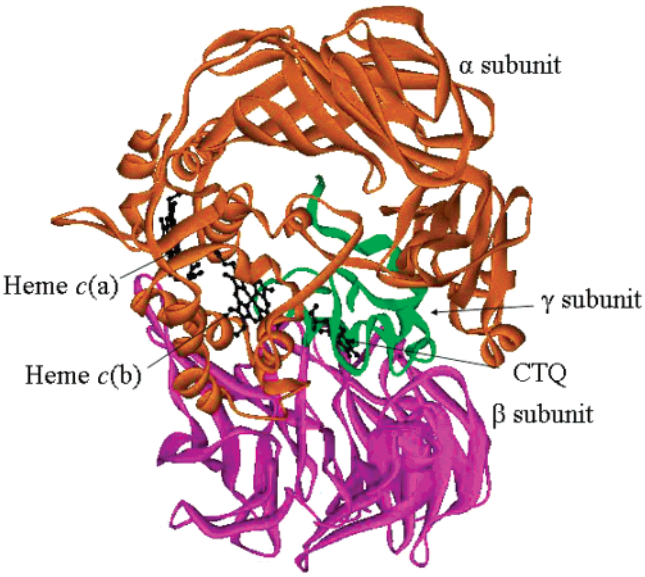

FIGURE 2: Crystal structure of *P. denitrificans* QHNDH. Only the protein backbone is shown. The relative positions of three redox centers are shown in a ball-and-stick model and colored black. The coordinates for this structure are available as PDB entry 1JJU (*5*).

of an orthoquinone-modified tryptophan ($Trp43_\gamma$) side chain covalently linked to a nearby cysteine side chain ($Cys37_\gamma$). In addition to CTQ, the γ subunit also contains three novel thioether cross-links that are formed between a Cys sulfur and either the β- or the γ-methylene carbon of an Asp or Glu residue. The largest α subunit is a 489-residue, four-domain polypeptide chain, which contains two heme *c* cofactors. Heme *c*(a) is solvent-accessible and has His and Met as the axial ligands. Heme *c*(b) is fully buried in the α subunit and located between CTQ and heme *c*(a). It has bis-axial His ligands. Both α and γ subunits sit on the surface of a 337-residue β subunit that forms part of the enzyme active site (*5*) (Figure 2). Because of the presence of three redox centers in QHNDH, it is difficult to measure the E_m value of each individual redox center in the intact protein. This is especially true for CTQ because of its relatively small extinction coefficient (7000 M^{-1} cm^{-1} at 380 nm) (*7*). Its spectrum is completely concealed by the heme spectra (ϵ = 227 000 M^{-1} cm^{-1} at 409 nm) (*2*). The E_m values of the three redox centers in QHNDH were determined by mediator-assisted continuous-flow column electrolytic spectroelectrochemistry to be CTQ = +65 mV (two-electron couple), heme *c*(b) = +149 mV, and heme *c*(a) = +235 mV (*7*). The value for CTQ was determined from the isolated γ subunit after dissociation from the protein (*7*). Given the configuration of the redox centers in QHNDH, at least four distinct reactions must occur upon the binding of substrate to the active site: (i) substrate oxidation by CTQ, (ii) ET from substrate-reduced CTQ to heme *c*(b), (iii) ET from heme *c*(b) to heme *c*(a), and (iv) ET from half-oxidized semiquinone CTQ to heme *c*(b). In the presence of its electron acceptor, intermolecular ET from heme *c*(a) to cytochrome *c*-550 will also occur. Thus, QHNDH provides a very good system to study both intra- and interprotein ET between different and similar redox cofactors.

The structure of CTQ is similar to that of the tryptophan tryptophylquinone (TTQ) cofactor (Figure 1) of methylamine dehydrogenase (MADH) (*8*, *9*). It is expressed in several bacteria, including *P. denitrificans*, when cells are grown on methylamine as a carbon source (*10*). QHNDH and MADH each catalyze an oxidative deamination reaction, however, they have very different overall structures. MADH is an $\alpha_2\beta_2$ heterotetramer that contains two identical active sites, each with TTQ as its only cofactor (*9*). QHNDH is a heterotrimer with one CTQ-containing active site and two hemes. Genetic analysis also suggests that the mechanisms of biosynthesis of the TTQ and CTQ cofactors are different. The biosynthesis of MADH in *P. denitrificans* requires four genes in addition to the structural genes *mauA* and *mauB* (*11*). Biosynthesis of QHNDH requires at least one extra gene (*5*), and it is different from those required for MADH biosynthesis. Moreover, in MADH, the TTQ-containing β subunit gene has a 57-amino acid long signal sequence that is believed to be important in TTQ biosynthesis (*12*), but for QHNDH the gene encoding the CTQ-containing γ subunit has no signal sequence (*5*).

Similarities of cofactor structure suggest that CTQ and TTQ may react with amine substrates by similar mechanisms. However, the different overall structures of QHNDH and MADH, additional redox centers in QHNDH, and apparent differences in the mechanism of cofactor biogenesis suggest that their respective reaction mechanisms may be different. Because of the relatively low extinction coefficient of CTQ as compared with the hemes of QHNDH, it has not been possible to directly monitor changes in its redox state during catalysis. In this paper, we report for the first time single-turnover transient kinetic studies of the reaction of QHNDH with substrate amines. These results together with those of steady-state kinetic, kinetic isotope effect, and isotope labeling studies are used to propose kinetic and chemical reaction mechanisms for QHNDH. These mechanisms are discussed in the context of the crystal structures of QHNDH and phenylhydrazine (Phz)-bound QHNDH.

EXPERIMENTAL PROCEDURES

Materials. Growth of *P. denitrificans* (ATCC 13543) and purification of QHNDH were as previously reported (*2*). Oxidized QHNDH was generated by incubation with potassium ferricyanide followed by dialysis to remove excess ferricyanide. QHNDH concentration was determined from the extinction coefficient of 227 000 M^{-1} cm^{-1} at 408 nm (*2*). CD_3NH_3·HCl, *n*-$C_4D_9NH_3$·HCl, and $C_6D_5CD_2NH_3$·HCl were obtained from C/D/N Isotopes (Quebec, Canada). Stereospecifically deuterium-labeled 2-phenylethylamines were synthesized as described below.

Kinetic Studies. Stopped-flow kinetic experiments were performed using an On-line instruments RSM16 stopped-flow rapid scanning spectrophotometer (OLIS, Bogart, GA). One syringe contained oxidized QHNDH, and the other contained the amine substrate. QHNDH was the limiting reactant with its concentration fixed at 1 μM. All experiments were performed at 30 °C in 0.01 M potassium phosphate, pH 7.5. Reactions were monitored at wavelengths between 380 and 620 nm. Details of the method of data analysis have been previously described (*13*). The concentration dependence of the reaction was analyzed using the simple kinetic model shown in eqs 1 and 2. For substrates with a high affinity for QHNDH ($K_d < 1$ μM), k_3 was

$$\mathrm{QHNDH_{ox}} + \mathrm{amine} \overset{K_d}{\rightleftharpoons} \mathrm{QHNDH_{ox}/amine} \overset{k_3}{\underset{k_4}{\rightleftharpoons}} \mathrm{QHNDH_{red}/product} \quad (1)$$

$$k_{obs} = k_4 + k_3[\mathrm{amine}]/(K_d + [\mathrm{amine}]) \quad (2)$$

determined from the rate at a saturating amine concentration (500 μM). This is valid since under all conditions that have been examined the value for k_4 is zero. Steady-state kinetic assays were performed in 0.01 M potassium phosphate, pH 7.5, at 30 °C as described previously (*2*). The assay mixture contained 16 nM QHNDH, saturating concentrations of amine substrate, 4.8 mM phenazine ethosulfate (PES) or methosulfate (PMS), and 170 μM 2,6-dichlorophenolindophenol (DCIP). The reaction was monitored at 600 nm to determine the rate of reduction of DCIP.

Synthesis of Chiral Deuterated Substrates. (*R*)-[1-^{2}H]-2-Phenylethylamine was prepared by decarboxylation of L-phenylalanine in D_2O with *Streptococcus faecalis* tyrosine decarboxylase (Sigma) (*14*). Solvent-exchangeable hydrogen atoms in sodium phosphate buffer (2 mmol, adjusted to pH 5.5) and L-phenylalanine (330 mg, 2 mmol) were exchanged with deuterium by repeated evaporation and dissolving in D_2O (5 mL × 3). The mixture was redissolved in 10 mL of D_2O and incubated with tyrosine decarboxylase (36 mg, 12.5 units) and pyridoxal 5′-phosphate (1 mg) at 37 °C for 3 days. The mixture was then made alkaline by the addition of 0.1 M NaOH, and the product amine was extracted with $CHCl_3$. Yield, 29 mg (12%); ^{2}H content by MS, monoderterated/dideuterated = 97:3; ^{1}H NMR ($CDCl_3$), 1.3 ppm (s, 2H), 2.74 ppm (d, J = 6.6 Hz, 2H), 2.95 ppm (m, 1H), 7.2−7.3 ppm (m, 5H).^{1}H NMR spectra were recorded with a JEOL-JNM-EX-270 at 270 MHz.

For synthesis of (*S*)-[1-^{2}H]-2-phenylethylamine, DL-[2-^{2}H]-phenylalanine was first prepared by nonenzymatic racemization of L-phenylalanine (1.3 g, 8 mmol) with pyridoxal hydrochloride (0.16 g, 0.8 mmol) in 10 mL of D_2O containing NaOD (16 mmol). The reaction mixture was refluxed for 2 h, freeze-dried, and refluxed again for 2 h in 10 mL of D_2O. A crystalline mass that precipitated on acidification (∼pH 5) of the mixture with 0.1 M HCl in an ice bath was collected by filtration and successively washed with cold water and methanol. After treatment with activated carbon, crystallization from methanol afforded the racemic [2-^{2}H]-phenylalanine with yield, 0.63 g (47%); ^{2}H content by ^{1}H NMR, 99%; ^{1}H NMR (D_2O), 2.82−2.98 ppm (AB system, J = 13.5 Hz, 2H), 7.3−7.4 ppm (m, 5H). (*S*)-[1-^{2}H]-2-Phenylethylamine was produced by enzymatic decarboxylation of DL-[2-^{2}H]-phenylalanine (330 mg, 2 mmol) in H_2O as described previously for synthesis of (*R*)-[1-^{2}H]-2-phenylethylamine with yield, 30 mg (12.5%); ^{2}H content by MS, monoderterated/dideuterated = 99:1; ^{1}H NMR ($CDCl_3$), 1.3 ppm (s, 2H), 2.74 ppm (d, J = 6.6 Hz, 2H), 2.95 ppm (m, 1H), 7.2−7.3 ppm (m, 5H).

[1,1-$^2H_2$]-2-Phenylethylamine was synthesized by reduction of phenylacetonitrile (1.0 g, 8.5 mmol) dissolved in ice-cooled THF (5 mL) with lithium aluminum deuteride (395 mg, 9.4 mmol). The mixture was refluxed overnight. After cooling on ice, ether (5 mL), H_2O (0.4 mL), and 15% (w/v) NaOH (0.4 mL) were added successively. After filtration, the product was extracted with ether and purified by distillation; yield, 68 mg (7%); ^{2}H content by MS, 99%; ^{1}H NMR ($CDCl_3$), 1.4 ppm (s, 2H), 2.74 ppm (s, 2H), 7.2−7.3 ppm (m, 5H). The ^{2}H-labeled 2-phenylethylamines were converted to sulfate salts by precipitating with sulfuric acid in methanol.

Stereoselectivity Studies. The QHNDH reaction with ^{2}H-labeled substrates was performed at 30 °C for 10 min in 0.1 M potassium phosphate, pH 7.5, containing 0.1 mM (*R*)- or (*S*)-[1-^{2}H]-2-phenylethylamine, 0.058 μM enzyme (0.018 U), and an electron acceptor (either 1 mM $K_3Fe(CN)_6$ or 1 mM PMS plus 50 μM DCIP) in a total volume of 1.0 mL. The product aldehyde was extracted with 500 μL of ethyl acetate and analyzed by GC-MS with a Shimadzu GC-17A gas chromatograph equipped with a capillary column DB-5MS (J & W Scientific, Inc.) and a Shimadzu GCMS-QP5050A mass spectrometer measuring in an m/z range of 50−200.

Stereospecificity for α-H abstraction from the substrate was also analyzed after the product aldehyde was converted into the corresponding alcohol by the coupling reaction with alcohol dehydrogenase. The reaction mixture (total volume, 1.0 mL), containing 0.1 M potassium phosphate, pH 7.5, 0.1 mM (*R*)- or (*S*)-[1-^{2}H]-2-phenylethylamine, 0.039 μM QHNDH (0.012 U), 2 mM $K_3Fe(CN)_6$, 0.2 mM NADH, and 0.23 U of equine liver alcohol dehydrogenase (Sigma), was incubated at 30 °C for 10 min. The alcohol (2-phenylethanol) was extracted with ethyl acetate and analyzed by GC-MS, as described previously.

Molecular Modeling. Model building of the 2-phenylethylamine-CTQ complex of QHNDH was performed using the commercial software package Insight II, version 98 (Accelrys Inc., San Diego, CA) run on a UNIX workstation (Silicon Graphics Inc., Mountain View, CA) with the X-ray crystal structure of the Phz-CTQ complex of QHNDH (*15*) (PDB entry 1PBY) as an initial structure. First, the model of 2-phenylethylamine bound to the C_6 carbonyl group of CTQ was constructed manually using the Builder module by replacing the Nβ atom of Phz with a carbon atom and inserting another methylene group to make the phenylethyl moiety. Two hydrogen atoms were also generated at the Cα position. Then, energy minimization was carried out using the Discover_3 module for the zone within 6 Å from CTQ under a constant valence force field, with the structure of the outside region (> 6 Å from CTQ) being fixed.

RESULTS

Three redox centers are present in QHNDH. To achieve ET from substrate to heme *c*(a), a minimum of four reaction

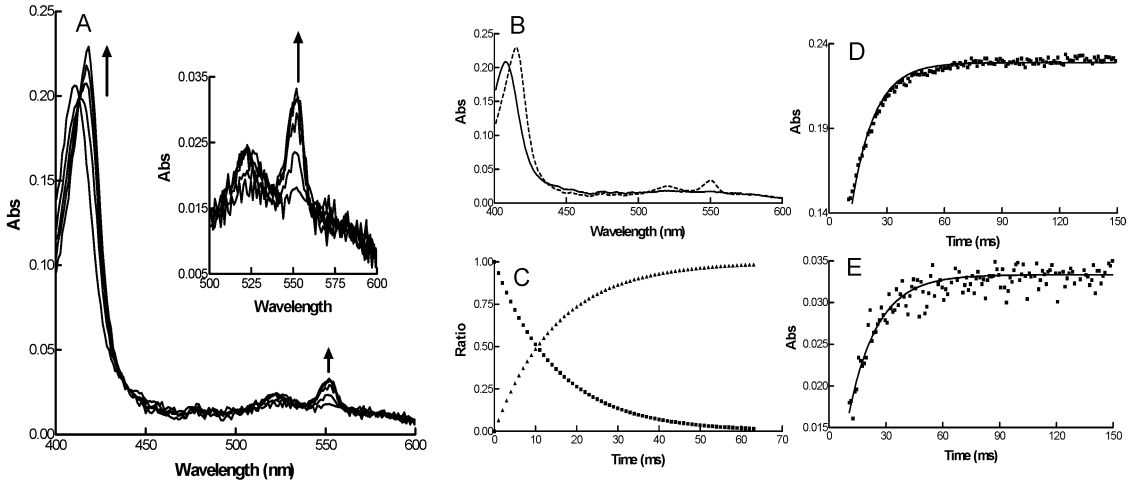

FIGURE 3: Reaction of oxidized QHNDH with methylamine. (A) The spectral changes associated with the reaction. Spectra were recorded every millisecond. Those, which are displayed, were recorded after 5, 13, 21, 29, and 74 ms. Arrows indicate the direction of the spectral changes. (B) Calculated spectra of the initial (solid line) and final (dashed line) absorbing species. These are essentially identical to those of fully oxidized and reduced QHNDH, respectively. (C) The change of the relative amounts of the two species shown in panel B with time. (D) The change of absorbance at 412 nm with time. (E) The change of absorbance 552 nm with time. The data in panels D and E were fit to the equation $Y = a_0 \exp(-k_{obs}t) + c$.

$$\begin{aligned}
&\text{substrate} + \text{CTQ}_{\text{oxidized}} - \text{heme } c(\text{b})_{\text{oxidized}} - \\
&\qquad\qquad \text{heme } c(\text{a})_{\text{oxidized}} \rightarrow \\
&\text{CTQ}_{\text{reduced}} - \text{heme } c(\text{b})_{\text{oxidized}} - \text{heme } c(\text{a})_{\text{oxidized}} \rightarrow \\
&\text{CTQ}_{\text{semiquinone}} - \text{heme } c(\text{b})_{\text{reduced}} - \text{heme } c(\text{a})_{\text{oxidized}} \rightarrow \\
&\text{CTQ}_{\text{semiquinone}} - \text{heme } c(\text{b})_{\text{oxidized}} - \text{heme } c(\text{a})_{\text{reduced}} \rightarrow \\
&\text{CTQ}_{\text{oxidized}} - \text{heme } c(\text{b})_{\text{reduced}} - \text{heme } c(\text{a})_{\text{reduced}} \qquad (3)
\end{aligned}$$

steps are necessary (eq 3). The spectral changes that occur on mixing substrate with QHNDH are shown in Figure 3. Only the spectral changes of heme moieties of QHNDH are observable. This is because of the large extinction coefficient of the hemes as compared with that of CTQ (*2*, *7*). The spectral change of QHNDH reflects the complete reduction of the two heme *c* groups. The data may be fit to a single exponential that represents the rate-limiting step in a substrate-dependent reduction of hemes in QHNDH. From these data alone, one cannot determine which reaction in eq 3 is rate-limiting. To determine this, experiments were performed with alternative amine substrates and deuterium-labeled substrates.

The rate of substrate-dependent heme reduction varies considerably depending upon the substrate (Table 1). The reaction rate of QHNDH with butylamine is 3-fold faster than that with methylamine and 12-fold faster than that with 2-phenylethylamine. According to the model described in eq 3, using a different substrate should only influence the first step in the reaction, the reduction of CTQ by the substrate. The substrate is not involved in any of the subsequent ET steps. These data suggest that CTQ reduction is the rate-limiting step in the single-turnover of the substrate-dependent reduction of heme in QHNDH.

Of the substrates tested, only methylamine exhibited a weak enough affinity for QHNDH to be able to determine its K_d from the concentration dependence of its reaction rate. The K_d value of 1.5 mM is similar to the previously reported steady-state K_m value of 1.3 mM (*2*). The very low K_d values

Table 1: Kinetic Parameters for Amine-Dependent Reduction of Heme in Single-Turnover Experiments

substrate	K_d (μM)	$^{H}k_3$ (s^{-1})	$^{D}k_3$ (s^{-1})	$^{H}k_3/^{D}k_3$
methylamine (CD_3NH_3)[a]	1500 ± 60	71.5 ± 1.5	13.5 ± 0.1	5.3 ± 0.1
butylamine (n-$C_4D_9NH_3$)	<1	188 ± 11	49 ± 5	3.9 ± 0.5
benzylamine ($C_6D_5CD_2NH_3$)	<1	162 ± 12	19 ± 0.6	8.5 ± 0.7
2-phenylethylamine ($C_6H_5CH_2CD_2NH_3$)	<1	16.9 ± 1.0	16.2 ± 1.0	1.05 ± 0.09

[a] The chemical formulas for the deuterated substrates are given in parentheses.

for butylamine, benzylamine, and 2-phenylethylamine are also consistent with the previously reported steady-state K_m values of <1 μM for these substrates (*2*). This suggests that the QHNDH active site has a much higher affinity for large and bulky amines than for small amines. It is interesting to note that while the K_d for methylamine is over 1000-fold greater than those of other amines, the rate constant for QHNDH reduction by methylamine is only 2.3-fold less than that of butylamine and 4.5-fold greater than that of 2-phenylethylamine.

If substrate oxidation is linked to CTQ reduction and is indeed the rate-limiting step in the substrate-dependent reduction of heme in QHNDH, then it may be possible to observe a deuterium KIE. For example, in TTQ-dependent amine dehydrogenases, the reduction of TTQ by substrate is concomitant with abstraction of a methyl proton by an active-site residue (*16*, *17*). If such a proton-transfer step is associated with the rate-limiting step in QHNDH reduction, then a KIE may be observed. The reaction rates of QHNDH with deuterated butylamine, benzylamine, 2-phenylethylamine, and methylamine were determined (Table 1). The reactions with methylamine, butylamine, and benzylamine each exhibit a significant primary KIE, which suggests that a proton-transfer reaction is at least partially rate-limiting for the substrate-dependent reduction of heme in QHNDH. In contrast, a primary KIE was not observed for the reaction

Table 2: Steady-State Kinetic Parameters for the Reaction of QHNDH with Amines and Artificial Electron Acceptors

substrate	$^{H}k_{cat}$ (s^{-1})	$^{D}k_{cat}$ (s^{-1})	$^{H}k_{cat}/^{D}k_{cat}$
butylamine (n-$C_4D_9NH_3$)[a]	5.8 ± 0.2	3.8 ± 0.1	1.5 ± 0.1
benzylamine ($C_6D_5CD_2NH_3$)	3.8 ± 0.2	2.5 ± 0.1	1.5 ± 0.1
2-phenylethylamine ($C_6H_5CH_2CD_2NH_3$)	3.1 ± 0.2	2.5 ± 0.1	1.2 ± 0.1

[a] The chemical formulas for the deuterated substrates are given in parentheses.

Table 3: Stereospecificity of α-H Abstraction from 2-Phenylethylamine

substrate	electron acceptor	deuterium content (%)[a]	
		aldehyde	alcohol
(*R*)-[1-^{2}H]-2-phenylethylamine	$K_3Fe(CN)_6$	99.7	99.7 ± 0.24[b]
	PMS/DCIP	99.1 ± 0.16[b]	Nd[c]
(*S*)-[1-^{2}H]-2-phenylethylamine	$K_3Fe(CN)_6$	22.2	18.6 ± 0.26[b]
	PMS/DCIP	20.5 ± 2.26[b]	Nd[c]

[a] Calculated from the relative heights of $[M^+]$ peaks of the product aldehyde or alcohol, which were corrected for contribution of $[M^+ - 1]$ and $[M^+ + 1]$ peaks using the values for the products from unlabeled substrate ($[M^+ - 1]/[M + 1] = 0.003$, $[M^+ + 1]/[M + 1] = 0.089$). [b] Standard deviation ($n = 4$). [c] Nd, not determined due to nonenzymatic reduction of PMS/DCIP by NADH.

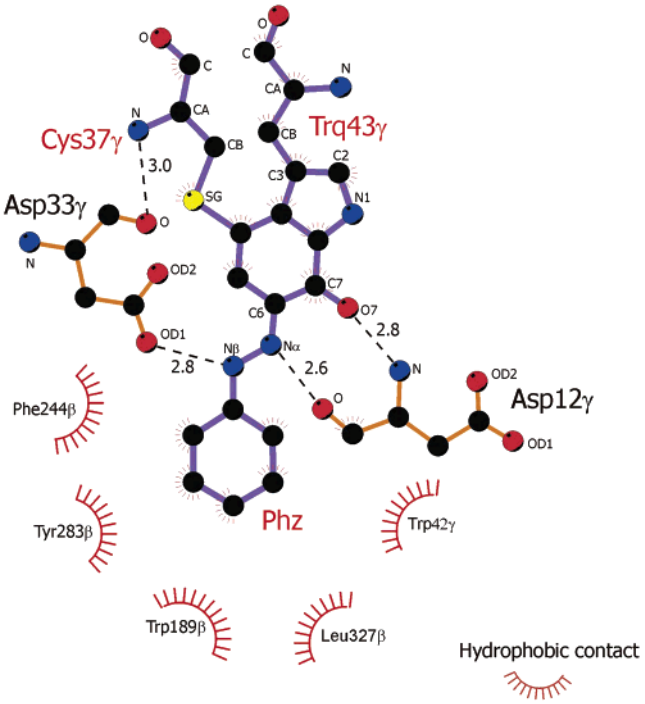

FIGURE 4: Schematic representation of the active site structure of Phz-inhibited QHNDH. This diagram was prepared using the LIGPLOT program (*22*). The coordinates for this structure are available as PDB entry 1PBY (*15*).

with 2-phenylethylamine. Furthermore, the rate of reaction of the unlabeled 2-phenylethylamine is much slower than the rates with unlabeled butylamine, benzylamine, and methylamine (16 s^{-1} as compared with 190, 162, and 72 s^{-1}). These results suggest that in the 2-phenylethylamine reaction, a different reaction step is rate-limiting than the proton-transfer step that is rate-limiting for the reaction with the other amines. That is why no KIE was observed for 2-phenylethylamine, and it follows that the rate of the actual rate-limiting step for QHNDH reduction by 2-phenylethylamine is the observed rate of 16 s^{-1}.

Since KIEs were observed for the single-turnover reaction of QHNDH with butylamine and benzylamine, the steady-state reaction of QHNDH was also examined for possible KIEs (Table 2). No primary KIE was observed for the reaction with butylamine, benzylamine, or 2-phenylethylamine. Consistent with the lack of a KIE is the observation that the k_{cat} values are much smaller than the rate constants for the reduction of QHNDH in the single-turnover experiments. There was also little variation in k_{cat} with different substrates. These data indicate that there is a different rate-limiting step in the steady-state reaction than in the single-turnover reaction, most likely the reoxidation of QHNDH by the external electron acceptor.

Although 2-phenylethylamines did not exhibit a KIE, proton abstraction from the CTQ-bound substrate must occur as a part of the overall reaction. To investigate whether this step is stereoselective, reactions of QHNDH were examined with 2-phenylethylamines stereospecifically deuterium-labeled at the α-carbon. ^{2}H contents in the product aldehydes and those converted into the corresponding alcohols were measured (Table 3). With (*R*)-[1-^{2}H]-2-phenylethylamine as substrate, the deuterium label was almost exclusively retained in the aldehyde or alcohol regardless of external electron acceptors (ferricyanide or PMS/DCIP), suggesting that the enzyme stereospecifically abstracts the pro-*S* hydrogen from the α-carbon of 2-phenylethylamine. However, the label was not completely lost when (*S*)-[1-^{2}H]-2-phenylethylamine was used but retained to about 20% in the product aldehyde or alcohol. Thus, while QHNDH does stereospecifically abstract the (*S*)-^{1}H atom in the (*R*)-[1-^{2}H]-substrate, the stereoselectivity decreases when the hydrogen atom to be abstracted is deuterium-labeled; 20% of the lighter atom (^{1}H vs ^{2}H) is abstracted even in the *R*-configuration. This small but noteworthy discrepancy of stereoselectivity derived from the ^{2}H-labeling of either one of the two enantiotopic hydrogen atoms may be explained by their relatively similar distances from the putative catalytic base (Asp33$_\gamma$) in the CTQ-bound substrate (discussed later).

The crystal structure of the Phz-inactivated QHNDH (Figure 4) (*15*) may be used to structurally interpret the incomplete stereoselectivity that is observed with chiral deuterated 2-phenylethylamines. The CTQ-bound 2-phenylethylamine substrate was modeled using the coordinates of the Phz-inhibited QHNDH (*15*). Energy minimization for the model caused no significant conformational changes of residues located within 6 Å from CTQ (Figure 5). In the final model, the phenyl ring of 2-phenylethylamine was well-accommodated in a hydrophobic pocket made up of several residues including Phe244$_\beta$, Tyr283$_\beta$, Trp42$_\gamma$, Trp189$_\beta$, and Leu327$_\beta$ (Figure 6). Residues around the entrance of the hydrophobic pocket (Phe244$_\beta$, Tyr283$_\beta$, and Trp42$_\gamma$) moved slightly to close the pocket, and those around the bottom of the pocket (Trp189$_\beta$, Phe85$_\beta$, and Leu327$_\beta$) moved to deepen the pocket (Figure 5), so that the phenyl ring of 2-phenylethylamine appears to be more tightly held inside the pocket than that of phenylhydrazone. As expected from the results of stereochemical analysis described previously, the pro-*S* hydrogen atom had a shorter distance (2.5 Å) than the pro-*R*

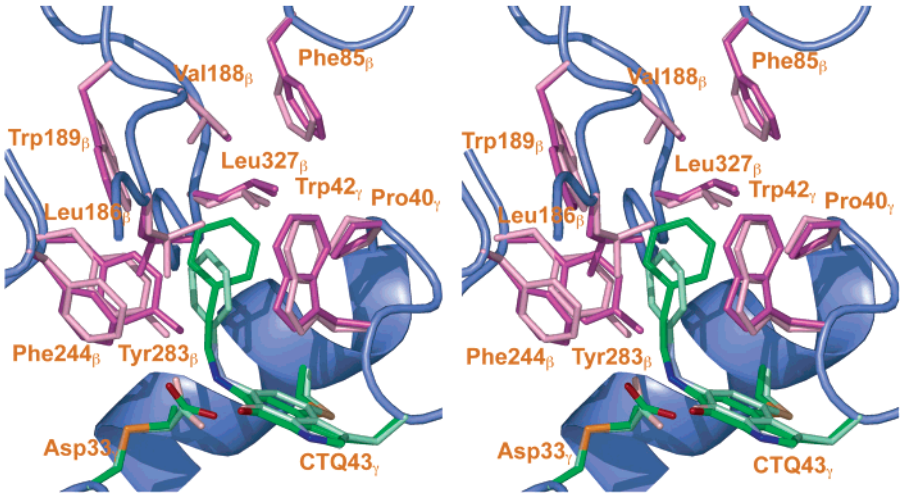

FIGURE 5: Stereo diagram of the modeled 2-phenylethylamine-CTQ complex superimposed on the crystal structure of the Phz-bound QHNDH. The main and side chains are shown in ribbon and stick models, respectively. Phz and 2-phenylethylamine are also shown in stick models. Residues in the substrate complex and those in the Phz complex are colored dark and light, respectively. This diagram was prepared using the PyMOL molecular graphics system (DeLano Scientific, San Carlos, CA).

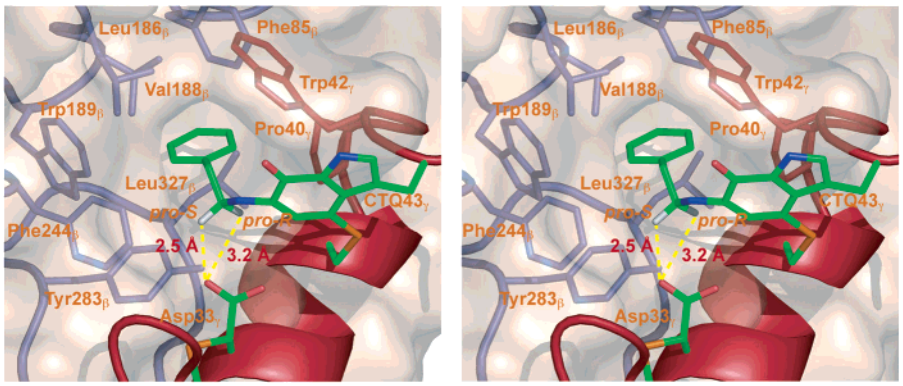

FIGURE 6: Stereo diagram of the phenyl ring of 2-phenylethylamine accommodated in the hydrophobic pocket. Residues of β and γ subunits are shown by gray and red sticks, respectively, except for CTQ, Asp33$_\gamma$, and 2-phenylethylamine, which are shown by green sticks. The two enantiotopic hydrogen atoms generated by computer are also shown with their distances to the nearest carboxyl oxygen atom of Asp33$_\gamma$, as is the surface of nearby hydrophobic residues in half-transparent gray. This diagram was prepared using the PyMOL molecular graphics system (DeLano Scientific, San Carlos, CA).

hydrogen atom (3.2 Å) to the OD1 carboxyl oxygen of Asp33$_\gamma$ (Figure 6), corroborating the high pro-*S* preference for proton abstraction. Furthermore, when the carboxyl group of Asp33$_\gamma$ is allowed to rotate freely around the $C_\alpha-C_\beta$ bond in the model, the shortest distances from the pro-*S* and pro-*R* hydrogen atoms to the carboxyl oxygen atom are estimated as 2.5 and 2.9 Å, respectively. This 0.4 Å difference is small enough to explain the incomplete stereoselectivity of proton abstraction described earlier.

DISCUSSION

The catalytic and ET properties of the TTQ-dependent amine dehydrogenases, MADH and aromatic amine dehydrogenase (AADH), have been extensively studied (*8*, *17*). However, the characterization of QHNDH is much more difficult. MADH and AADH possess only TTQ as a cofactor, and the electron acceptor for each enzyme is another protein. Thus, it is possible to study the catalytic and ET reactions of TTQ in these two amine dehydrogenases separately. For QHNDH, the active site with CTQ and its initial electron acceptors, hemes *c*(a) and *c*(b), are present in the same protein. Thus, ET occurs immediately after the catalysis. Moreover, due to the spectral overlap of different redox centers and the relatively low absorbance of CTQ, it is not possible to directly monitor changes in the redox state of the quinone cofactor during the overall reaction. From the results obtained in this study, it is now possible to propose chemical and kinetic reaction mechanisms for QHNDH.

The crystal structure of Phz-inhibited QHNDH (*15*) (Figure 4) provides structural insight into the roles of specific residues in the chemical reaction mechanism and substrate binding. A similar structure with Phz bound is available for a Phe55$_\alpha$ to Ala mutant of MADH that exhibits altered substrate specificity (*18*). However, Phz is not a good analogue of methylamine, which is the substrate for MADH. For QHNDH, Phz is a better structural analogue of its substrates, benzylamine and 2-phenylethylamine. The crystal structure of Phz-inhibited QHNDH indicates that the site of nucleophilic attack by the amine nitrogen is the C_6 of CTQ, which corresponds to the position of the reactive carbonyl of TTQ in MADH. It has not yet been proven, for any quinoprotein amine dehydrogenase, which residue is the one that abstracts the proton from the α-carbon of the bound substrate. The active sites in the structures of MADH from *P. denitrificans* and QHNDH from *P. denitrificans* are overlaid in Figure 7. Each contains two Asp residues in close

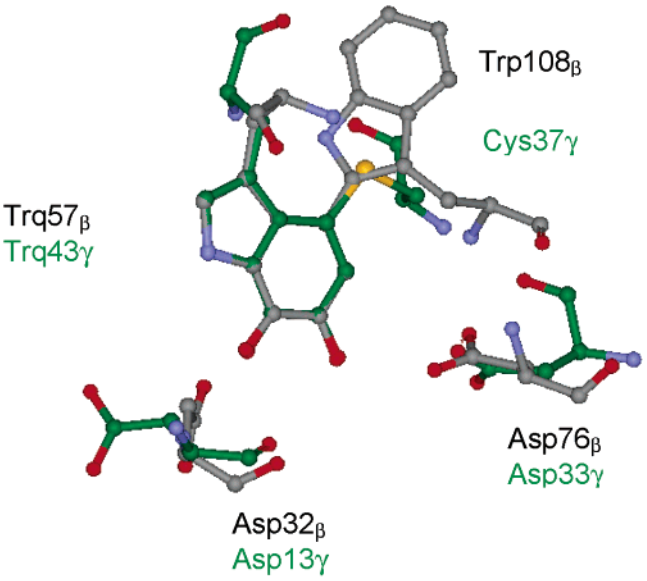

FIGURE 7: Overlay of tryptophylquinone cofactors and structurally conserved aspartic acid residues in the structures of MADH and QHNDH. The carbon atoms are colored green in the QHNDH structure and gray in the MADH structure. The labels corresponding to the QHNDH structure are also in green.

proximity to the active quinone carbonyl. Asp33$_\gamma$ of QHNDH and Asp76$_\beta$ of MADH have their side chains oriented toward the C_6 of the tryptophylquinone (Trq) moiety of the quinone cofactor. Unfortunately, it was not possible to determine the role in catalysis of Asp76$_\beta$ of MADH because site-directed mutagenesis of that residue resulted in undetectable levels of MADH production (*19*). Asp13$_\gamma$ of QHNDH and Asp32$_\beta$ of MADH each has its side chain pointing away from the quinone, but each has its main chain carbonyl oxygen pointed toward the C_6. This similarity is remarkable given the very different overall structures of MADH and QHNDH. The MADH active site is relatively spacious considering that its substrate is methylamine. Since the substrates of QHNDH are primary amines with either long aliphatic carbon chains or bulky aromatic rings, the positioning of substrate in the QHNDH active site will be more restricted than that of methylamine in MADH. It can be seen in Figure 4 that the phenylhydrazone ring is positioned close to the C_6 of CTQ in a hydrophobic pocket, which is formed by residues Phe244$_\beta$, Tyr283$_\beta$, Leu327$_\beta$, Trp189$_\beta$, and Trp42$_\gamma$. The side chain of Asp33$_\gamma$ is close to the β-nitrogen of the phenylhydrazone, which is the counterpart of the α-carbon of the substrate. On the basis of this structure and molecular modeling studies (Figure 6), one may conclude that Asp33$_\gamma$ is most likely to be the residue that performs the proton abstraction. A very recent paper on the crystal structure of QHNDH from *Ps. putida* bound with *p*-nitrophenylhydrazine (*20*) also supports the assignment for Asp33$_\gamma$ to be the catalytic base.

In the steady-state assay, QHNDH exhibits a similar k_{cat} with all substrates. The k_{cat} values are much smaller than the rate constants obtained in the single-turnover kinetic studies. Moreover, there is no significant KIE observed in the steady-state k_{cat} values for all substrates. It was also previously reported that QHNDH shows different k_{cat} values in the steady-state assay when different electron acceptors are used (*2*). The explanation for these data is that the rate-limiting step in the steady-state is the ET from heme *c*(a) to

CTQ(oxidized)·Heme *c*(b)(oxidized)·Heme *c*(a)(oxidized) + substrate

⇅ K_d for substrate

Substrate-CTQ(oxidized)·Heme *c*(b)(oxidized)·Heme *c*(a)(oxidized)

⇅ k_3 (CTQ reduction)
Rate-limiting step in the single-turnover reaction with butylamine and methylamine

Product-CTQ(reduced)·Heme *c*(b)(oxidized)·Heme *c*(a)(oxidized)

⇅ k_5 (product release)
Rate-limiting step in the single-turnover reaction with 2-phenylethylamine

CTQ(reduced)·Heme *c*(b)(oxidized)·Heme *c*(a)(oxidized) + product

⇅ k_7 (first internal electron transfer)

CTQ(semiquinone)·Heme *c*(b)(reduced)·Heme *c*(a)(oxidized)

⇅ k_9 (second internal electron transfer)

CTQ(oxidized)·Heme *c*(b)(reduced)·Heme *c*(a)(reduced)

⇅ K_d for electron acceptor

CTQ(oxidized)·Heme *c*(b)(reduced)·Heme *c*(a)(reduced) + Acceptor(oxidized)

⇅ k_{13} (inter-molecular electron transfer to acceptor)
Rate-limiting in the steady-state reaction

CTQ(oxidized)·Heme *c*(b)(oxidized)·Heme *c*(a)(oxidized) + Acceptor(reduced)

FIGURE 8: Proposed kinetic mechanism for the steady-state reaction of QHNDH with amine substrates and an electron acceptor.

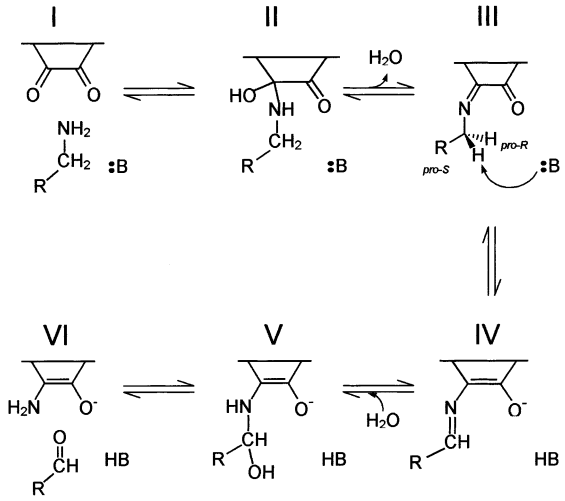

FIGURE 9: Proposed chemical reaction mechanism for the reduction of CTQ in QHNDH by amine substrates. Only the quinone portion of CTQ is shown.

the external electron acceptor. The overall kinetic reaction mechanism for QHNDH in the steady-state is summarized in Figure 8.

A chemical reaction mechanism for the reductive half-reaction of CTQ by substrate is proposed in Figure 9, which is similar to the proposed mechanisms of TTQ reduction by substrate in AADH (*17*) and MADH (*8*). The reaction is initiated by a nucleophilic attack by the amine nitrogen on the C_6 quinone carbonyl. This forms a carbinolamine intermediate (II) that loses water to form an imine intermediate (III). Then an active-site residue (most likely Asp33$_\gamma$) abstracts a proton from the α-carbon to form a carbanionic

intermediate concomitant with the reduction of the CTQ cofactor to form intermediate IV. Release of the product aldehyde occurs by hydrolysis of the newly formed imine bond between the α-carbon and the amino group. For the reduction of CTQ by methylamine, butylamine, and benzylamine, large primary KIEs were observed (Table 1). Thus, the reaction of CTQ with these substrates is rate-limited by the proton-transfer step in the formation of intermediate IV. For the reaction with 2-phenylethylamine, no primary KIE was observed, and the reaction rate was much smaller. With 2-phenylethylamine, therefore, the reaction must be rate-limited by another reaction step that precedes the relatively rapid ET reactions from reduced CTQ. This is most likely the product release step (see Figure 8). Previous studies with MADH and AADH have indicated that the rate-limiting step in the steady-state in their reactions is the hydrolysis of intermediate IV and release of the aldehyde product (*16*, *17*). It has also been shown with MADH that the rapid ET from intermediate VI to amicyanin is activated by the binding of another molecule of substrate in the active site (*21*). For QHNDH, it is possible that either hydrolysis of the imine intermediate or release of the aldehyde product from the active site may need to precede binding of another substrate molecule to the active site to activate the system for rapid ET. The modeling studies discussed earlier indicated that 2-phenylethylamine fits more tightly into the hydrophobic binding site than does Phz. This could explain the slower release of the 2-phenylethylamine-derived aldehyde product, relative to those derived from benzylamine and aliphatic amines.

The chemical reaction mechanism for 2-phenylethylamine is likely to be the same as that described in Figure 9. Even though proton transfer is not rate-limiting, that step must occur. In fact, the results with chiral deuterated 2-phenylethylamines proved that this reaction step not only occurs but is stereoselective, although the stereoselectivity decreases slightly when the abstracted hydrogen atom is deuterated. The decrease in stereoselectivity may be attributed to an intrinsic KIE in the proton-transfer step. Assuming that both of the enantiotopic α-hydrogen atoms of 2-phenylethylamine can be abstracted, but with much higher preference for the pro-*S* hydrogen, the percentage deuterium contents, R_R and R_S in the product aldehydes from (*R*)- and (*S*)-[1-^{2}H]-2-phenylethylamines, respectively, are given by eqs 4 and 5.

$$R_R = [k_{3,S}/(k_{3,S} + k_{3,R}/\mathrm{KIE})]100 \quad (4)$$

$$R_S = [k_{3,R}/(k_{3,S}/\mathrm{KIE} + k_{3,R})]100 \quad (5)$$

The rate constants for abstraction of the pro-*S* and pro-*R* protons of nonlabeled 2-phenylethylamine are $k_{3,S}$ and $k_{3,R}$, respectively (see Figure 8), and KIE is the intrinsic KIE for deuterium-labeled substrates. By applying experimentally determined deuterium contents in the product aldehydes (Table 3; averaged values, $R_R = 99.4$, $R_S = 21.4$) to eqs 4 and 5, KIE is calculated to be 6.7, comparable to the KIEs ($^Hk_3/^Dk_3$) of methylamine and benzylamine determined in the single-turnover experiments (Table 1). This large intramolecular KIE explains the deuterium retention in the product aldehyde. These equations also give a true pro-*S* selectivity, $k_{3,S}/(k_{3,S} + k_{3,R})$, of 0.96, which indicates that the true stereoselectivity is imperfect, although only slightly. The most likely explanation for the experimental observation that 20% of the lighter atom (^{1}H vs ^{2}H) is abstracted, even in the *R*-configuration, is that the distances separating the proton acceptor and each of the two enantiotopic α-hydrogen atoms are not significantly different. This is consistent with what was observed in the modeled 2-phenylethylamine-CTQ complex (Figure 6), in which the distances from the two enantiotopic α-hydrogen atoms to the putative catalytic base, Asp33$_\gamma$, differed by only 0.4 Å.

ACKNOWLEDGMENT

We thank Dr. Hideyuki Hayashi, Osaka Medical College, for helpful discussions.

REFERENCES

1. Adachi, O., Kubota, T., Hacisalihoglu, A., Toyama, H., Shinagawa, E., Duine, J. A., and Matsushita, K. (1998) *Biosci. Biotechnol. Biochem. 62*, 469−478.
2. Takagi, K., Torimura, M., Kawaguchi, K., Kano, K., and Ikeda, T. (1999) *Biochemistry 38*, 6935−6942.
3. Shinagawa, E., Matsushita, K., Nakashima, K., Adachi, O., and Ameyama, M. (1978) *Agric. Biol. Chem. 52*, 2255−2263.
4. Takagi, K., Yamamoto, K., Kano, K., and Ikeda, T. (2001) *Eur. J. Biochem. 268*, 470−476.
5. Datta, S., Mori, Y., Takagi, K., Kawaguchi, K., Chen, Z. W., Okajima, T., Kuroda, S., Ikeda, T., Kano, K., Tanizawa, K., and Mathews, F. S. (2001) *Proc. Natl. Acad. Sci. U.S.A. 98*, 14268−14273.
6. Satoh, A., Kim, J. K., Miyahara, I., Devreese, B., Vandenberghe, I., Hacisalihoglu, A., Okajima, T., Kuroda, S., Adachi, O., Duine, J. A., Van Beeumen, J., Tanizawa, K., and Hirotsu, K. (2002) *J. Biol. Chem. 277*, 2830−2834.
7. Fujieda, N., Mori, M., Kano, K., and Ikeda, T. (2002) *Biochemistry 41*, 13736−13743.
8. Davidson, V. L. (2001) *Adv. Protein Chem. 58*, 95−140.
9. Chen, L., Doi, M., Durley, R. C., Chistoserdov, A. Y., Lidstrom, M. E., Davidson, V. L., and Mathews, F. S. (1998) *J. Mol. Biol. 276*, 131−149.
10. Husain, M., and Davidson, V. L. (1987) *J. Bacteriol. 169*, 1712−1717.
11. van der Palen, C. J., Slotboom, D. J., Jongejan, L., Reijnders, W. N., Harms, N., Duine, J. A., and van Spanning, R. J. (1995) *Eur. J. Biochem. 230*, 860−871.
12. Chistoserdov, A. Y., and Lidstrom, M. E. (1991) *J. Bacteriol. 173*, 5909−5913.
13. Bishop, G. R., Brooks, H. B., and Davidson, V. L. (1996) *Biochemistry 35*, 8948−8954.
14. Bettersby, A. R., Chrystal, E. J., and Staunton, J. (1980) *J. Chem. Soc., Perkin Trans. 1*, 31−42.
15. Datta, S., Ikeda, T., Kano, K., and Mathews, F. S. (2003) *Acta Crystallogr. D*, in press.
16. Brooks, H. B., Jones, L. H., and Davidson, V. L. (1993) *Biochemistry 32*, 2725−2729.
17. Hyun, Y. L., and Davidson, V. L. (1995) *Biochemistry 34*, 816−823.
18. Sun, D., Chen, Z. W., Mathews, F. S., and Davidson, V. L. (2002) *Biochemistry 41*, 13926−13933.
19. Sun, D., Jones, L. H., Mathews, F. S., and Davidson, V. L. (2001) *Protein Eng. 14*, 675−681.
20. Satoh, A., Adachi, I., Tanizawa, K., and Hirotsu, K. (2003) *Biochim. Biophys. Acta 1647*, 272−277.
21. Davidson, V. L., and Sun, D. (2003) *J. Am. Chem. Soc. 125*, 3224−3225.
22. Wallace, A. C., Laskowski, R. A., and Thornton, J. M. (1995) *Protein Eng. 8*, 127−134.

BI035062R